

INFLUENCE OF SILICON AND PHOSPHORUS ON STRUCTURAL AND MAGNETIC PROPERTIES OF SYNTHETIC GOETHITE AND RELATED OXIDES

THOMAS G. QUIN,¹ GARY J. LONG,² CHRISTOPHER G. BENSON,²
STEPHEN MANN,³ AND ROBERT J. P. WILLIAMS¹

¹ Inorganic Chemistry Laboratory and the Chemical Crystallography Laboratory
Oxford University, Oxford OX1 3QR, United Kingdom

² Department of Chemistry, University of Missouri–Rolla
Rolla, Missouri 65401 and
Department of Physics, University of Liverpool
Liverpool L69 3BX, United Kingdom

³ School of Chemistry, University of Bath
Bath BA2 7AY, United Kingdom

Abstract—A series of synthetic goethites containing varying amounts of Si and P dopants were characterized by X-ray powder diffraction, electron diffraction, microbeam electron diffraction, and Mössbauer spectroscopy. Very low level incorporation produced materials having structural and spectral properties similar to those of poorly crystalline synthetic or natural goethite. At higher incorporation levels, mixtures of noncrystalline materials were obtained which exhibited Mössbauer spectra typical of noncrystalline materials mixed with a superparamagnetic component. Microbeam electron diffraction indicated that these mixtures contained poorly crystalline goethite, poorly crystalline ferrihydrite, and a noncrystalline component. If the material was prepared with no aging of the alkaline Fe³⁺ solution before the addition of Na₂HPO₄ or Na₂SiO₃, materials were obtained containing little if any superparamagnetic component. If the alkaline Fe³⁺ solution was aged for 48 hr before the addition, goethite nuclei formed and apparently promoted the precipitation of a superparamagnetic phase. The Mössbauer-effect hyperfine parameters and the saturation internal-hyperfine field obtained at 4.2 K were typical of those of goethite; however, the Mössbauer spectra indicated that the ordering temperature, as reflected in the relaxation rate and/or the blocking temperature, decreased with increasing incorporation of Si and P. The complete loss of crystallinity indicates that Si and P did not substitute for Fe, but rather adsorbed on crystal-growth sites, thereby preventing uniform crystal growth.

Key Words—Electron diffraction, Ferrihydrite, Goethite, Mössbauer spectroscopy, Phosphorus, Silicon, X-ray powder diffraction.

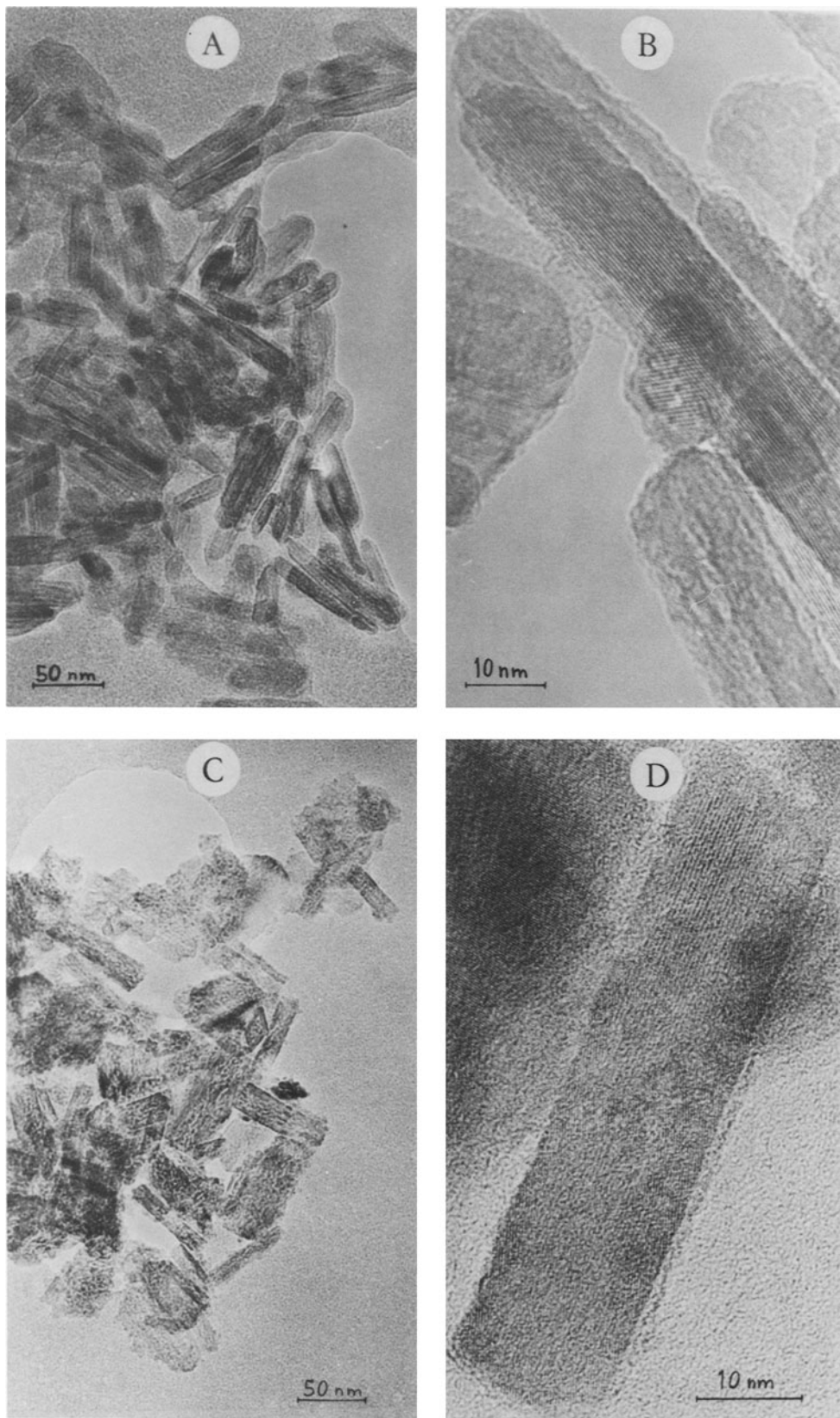
INTRODUCTION

Acicular crystals of goethite can be prepared by transformation of noncrystalline or poorly crystalline gels of ferrihydrite composition (Böhm, 1925; Schwertmann and Fischer, 1966; Atkinson *et al.*, 1968; Cornell and Schwertmann, 1979). Electron diffraction studies (Goltztaub, 1935; van Oosterhout, 1960; Cornell *et al.*, 1983) have shown that goethite crystals are commonly elongated in the [001] direction, although factors such as pH, temperature, and the presence of foreign elements in the synthetic system can influence the morphology of the final product. Synthetic goethites doped with Al have been widely studied (e.g., Fysh and Clark, 1982; Fysh and Fredericks, 1983; Murad and Schwertmann, 1983; Schulze, 1984; Mann, 1983). Al substitutes directly in goethite for Fe in octahedral sites because the ionic radius of Al (0.67 Å) (Shannon and Prewitt, 1969) is similar to that of Fe³⁺ (0.78 Å). Mössbauer spectroscopy (Taylor and Schwertmann, 1974; Murad and Schwertmann, 1983) have shown that Al substitution has the same effect on the magnetic prop-

erties of goethite as does poor crystallinity, namely, that it reduces the saturation internal hyperfine field.

Despite the fact that their octahedral ionic size (0.54 and 0.52 Å, respectively) argues against their incorporation into the goethite structure, Schwertmann and Thalmann (1976) and Koch *et al.* (1986) showed that Si and P affect the goethite crystallization process by stunting the growth of the acicular goethite crystals. The goal of the present investigation was to examine the influence of Si and P on the long-range crystalline and magnetic order of synthetic and natural solid iron oxides including goethite because iron oxides found both in clay minerals and biological substances (Mann, 1983; Mann *et al.*, 1986) must have been deposited in the presence of both these elements. To this end, goethite-like products were prepared by precipitating aged solutions of ferric nitrate, sodium phosphate, and sodium silicate at pH 13.5–14. The products were then examined by X-ray powder and electron diffraction, electron microscopy, and Mössbauer spectroscopy.

The term goethite is used in this report for materials



that were identified positively by X-ray powder or conventional electron diffraction methods. Materials which gave no characteristic X-ray powder diffraction patterns of goethite, but which gave microbeam electron diffraction patterns characteristic of goethite, ferrihydrite, and other iron oxide materials and which had H:Fe atomic ratios near that of theoretical goethite are referred to as mixtures. The name ferrihydrite is used herein for materials showing characteristic microbeam electron diffraction patterns and H:Fe ratios close to that of "theoretical" ferrihydrite, $5\text{Fe}_2\text{O}_3 \cdot 9\text{H}_2\text{O}$ (Towe and Bradley, 1967; Chukhrov, 1973; Russell, 1979).

EXPERIMENTAL

The goethites were prepared by the method described by Atkinson *et al.* (1968). In each experiment 10.1 g (0.025 mole) of $\text{Fe}(\text{NO}_3)_3 \cdot 9\text{H}_2\text{O}$ was placed in a polythene bottle and dissolved in 30–40 cm³ of distilled water. For pure goethite, sufficient aqueous NaOH was added to the ferric nitrate solution to give a pH of 10–11. After aging at $21^\circ \pm 3^\circ\text{C}$ for 50 hr some precipitation occurred giving a layer of slurry and a layer of brownish supernatant solution. The sample was then heated in an oven at $70^\circ \pm 3^\circ\text{C}$. After 17 hr, a thin layer of solid was observed beneath a clear, colorless, supernatant liquid.

Goethites incorporating Si and P were prepared by two methods. In method I, 10 cm³ of aqueous NaOH was added to the ferric nitrate solution, and the resulting alkaline solutions, having a pH of ~ 13.5 , were aged at $21^\circ \pm 3^\circ\text{C}$ for 48 hr. Different volumes of a 0.1 M Na_2HPO_4 or Na_2SiO_3 solution and 2.5 M NaOH solution were added until a pH of 13.5–14 was obtained. After vigorous agitation the samples were placed in a $70^\circ \pm 3^\circ\text{C}$ oven for 1–15 days until goethite precipitation appeared to be complete. Method II was identical except that the samples were heated at $70^\circ \pm 3^\circ\text{C}$ immediately after all solutions had been mixed. All preparations were then washed by repeated stirring with distilled water followed by centrifugation. The solid products were air dried at room temperature and characterized by elemental analysis (see Table 1).

The ratio of Fe to Si or P was determined by selected-area, energy-dispersive X-ray analysis (EDX) in a scanning electron microscope. The ratio of peak integrals was multiplied by a constant obtained from equivalent measurements on a known calibrant (Cheetham and Skarmulis, 1981). These results were related to the water content by atomic absorption analysis for Fe and classical chemical analysis for H (by heating to extract water, which was measured by quantitative chromatography).

For electron imaging and conventional diffraction a JEOL 100CX TEMSCAN electron microscope was used. This instrument is a conventional transmission electron microscope with added scanning coils. High-resolution imaging was achieved with a JEOL 200CX transmission electron microscope. A JEOL 2000FX instrument was used for microelectron diffraction, wherein the electron beam was focused onto a sample area of $3 \times 10^4 \text{ \AA}^2$. The specimens used for microscopy were prepared from finely ground material suspended in chloroform. One or two drops of the suspension were placed on carbon-coated, Formvar-covered, copper grids. X-ray powder diffraction (XRD) patterns were obtained by

Table 1. Characterization of synthetic goethite and composite products.

Preparation	Preparative method ¹	Initial dopant molar ratio ²	Mole ratio dopant per iron	Mole ratio water per iron ³	Composition ⁴ (%)	
					Goethite	Ferrihydrite
1	I	0	—	0.190	100	0
2	I	0.01	0.025 Si	0.010	100	0
3	I	0.02	0.040 Si	0.121	0	25
4	I	0.036	0.075 Si	0.327	10	0
5	I	0.021	0.084 Si	0.505	0	15
6	II	0.025	0.086 Si	0.158	20	30
7	II	0.025	0.106 Si	0.770	0	55
8	II	0.038	0.123 Si	0.460	5	25
9	I	0.02	0.007 P	0.155	100	0
10	II	0.012	0.035 P	0.185	80	20
11	II	0.03	0.036 P	0.388	35	25
12	I	0.033	0.058 P	0.744	10	25
13	I	0.038	0.068 P	0.484	10	25
14	II	0.03	0.082 P	0.539	0	15

¹ As defined in text under Experimental.

² In terms of the Si/Fe or P/Fe molar ratio.

³ In excess of the stoichiometric quantity in FeOOH.

⁴ As determined from microbeam electron diffraction, as explained in the Results section.

using a Stoe-Guinier camera, having a narrow-slit X-ray source and a highly reflective curved graphite monochromator for high-angular resolution. The Mössbauer spectra were measured on a Harwell constant-acceleration spectrometer which utilized a room-temperature, rhodium-matrix cobalt-57 source and which was calibrated at room temperature with natural abundance α -iron foil. All absorbers contained 19 mg/cm² of sample. Spectra were obtained at 4.2 K in a cryostat which placed the sample directly in liquid helium. Variable-temperature spectra were obtained in an Oxford Instruments flow cryostat. Spectral analysis was carried out by using either standard least-squares minimization techniques (Longworth, 1984) or standard procedures (Wivel and Mørup, 1981) for determining the distribution of hyperfine magnetic fields.

RESULTS

Analytical results

High- and low-incorporation ratios were obtained from both methods of preparation. Method II, in which all crystallization took place in the presence of Si or P, was used to obtain products incorporating more of these elements; however, as illustrated in Table 1, the ratios of Si or P to Fe in products prepared by this method do not correlate directly with the initial concentrations of the dopant solution. In general, higher initial dopant concentrations produced higher incorporation levels in the products. The water content, of ≤ 0.5 mole/Fe as determined by thermal gravimetric analysis, is listed in Table 1.

Figure 1. High-resolution electron micrographs of (A, B) synthetic goethite, preparation 1, and (C, D) preparation 2. In A and C, scale bar is $50 \times 10^{-3} \mu\text{m}$, in B and D, scale bar is $10 \times 10^{-3} \mu\text{m}$. In B the lattice-fringe separation is 4.5 Å; in D, it is 3.8 Å.

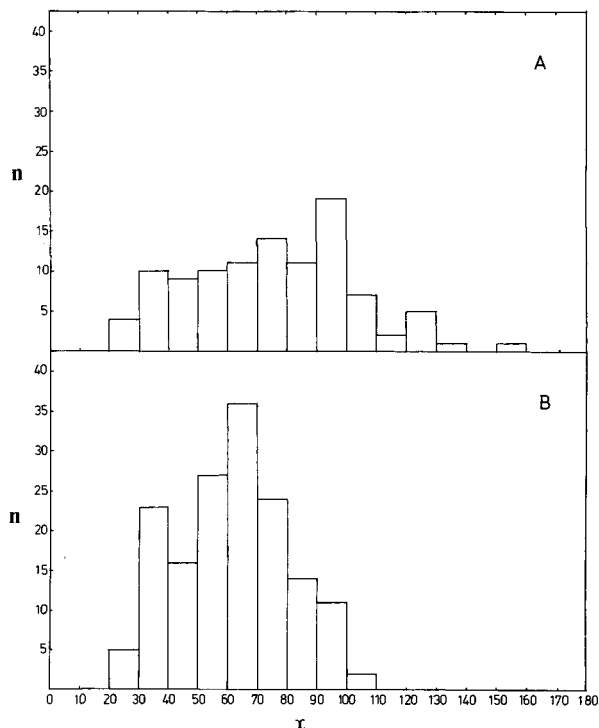


Figure 2. Distribution of crystal lengths in nanometers in (A) synthetic goethite, preparation 1, and (B) preparation 2, which is incorporated with 2.5 mole % Si relative to Fe.

Electron and X-ray powder diffraction

Both electron diffraction and XRD methods were used to evaluate the crystallinity and homogeneity of the products (Table 1). Single crystal electron diffraction patterns, characteristic of goethite, were displayed by preparation 1. In the products incorporating Si and P, only preparation 9 (containing <1% dopant) gave an XRD pattern of goethite. None of the other products produced either XRD or conventional electron diffraction patterns, indicating either very poor or non-existent crystallinity. Microbeam electron diffraction was then used to investigate the local crystalline order in the materials. In this technique (Quin, 1986) the electron beam spot size was reduced to a minimum diameter of about 200 Å and the diffraction pattern from the resulting area was observed. In this way a diffraction pattern could be obtained from a small selected area of the material. Microbeam electron diffraction, with its enhanced sensitivity, revealed varying proportions of poorly crystalline goethite and ferrihydrite, as well as nondiffracting material (see Table 1).

Transmission electron microscopy and diffraction

High- and low-resolution electron micrographs of each product were obtained in the transmission mode of the electron microscope. The degree of departure

from the typical acicular morphology of goethite increased as the degree of Si and P incorporation increased. Incorporation of 2.5 mole % Si resulted in a reduction of the crystal by ~18% and a stunting of the acicular morphology along the needle axis (Figure 1). This reduction in length and change in frequency distribution (Figure 2) indicate that growth was in part inhibited in the [001] crystal direction, which is parallel to the double chains of $\text{Fe}(\text{O},\text{OH})_6$ octahedra (Murad and Johnston, 1987). The preferential growth sites occur at the ends of the chains because the gaps present between these parallel chains (see Figure 9 of Murad and Johnston, 1987) make the plane normal to the [001] direction "rougher" on an atomic scale and, therefore, more energetically favorable for the adsorption of the Si and P. The morphology of the Si-containing sample (Figures 1C and 1D) was more regular than that of goethite (cf. Figures 1A and 1B), but the disorder in the lattice fringes (Figure 1D) indicates structural irregularities, such as stepping in the crystal surface. At higher incorporation levels crystallization was further inhibited such that a mixture of microcrystalline materials was obtained (see Table 1).

Mössbauer spectroscopy

Mössbauer spectra of acicular crystals of natural goethite from the Restormel mine, Cornwall, United Kingdom (Figure 3), can be compared with those of synthetic goethite (preparation 1, Figure 4). All natural samples are ordered at room temperature, but the line-widths of the magnetic sextets vary with the degree of crystallinity of the samples. The Restormel sample produced a spectrum virtually identical with those reported by Mørup *et al.* (1983). As expected, the synthetic goethite of preparation 1, which was less crystalline than the natural samples, produced a significantly broadened magnetic spectrum at room temperature. The saturation internal hyperfine field was essentially the same as that observed for the natural sample. The area-weighted average hyperfine parameters at selected temperatures for each preparation, resulting from the individual components shown in the illustrations, are presented in Table 2. The distribution in internal hyperfine fields was determined by the method of Wivel and Mørup (1981); the spectra were also fit to several magnetic sextets (Figures 5–13). The hyperfine parameters for the internal hyperfine-field distribution fits for all temperatures are given in Table 3, along with the percentage of non-ordered material.

At room temperature, only preparation 2 of the materials incorporating Si was ordered; it showed a broad distribution in the internal hyperfine fields, indicating a high level of crystal imperfection. At room temperature all other materials incorporated with Si showed quadrupole doublets, the magnetic hyperfine field having collapsed with the decrease in long-range magnetic

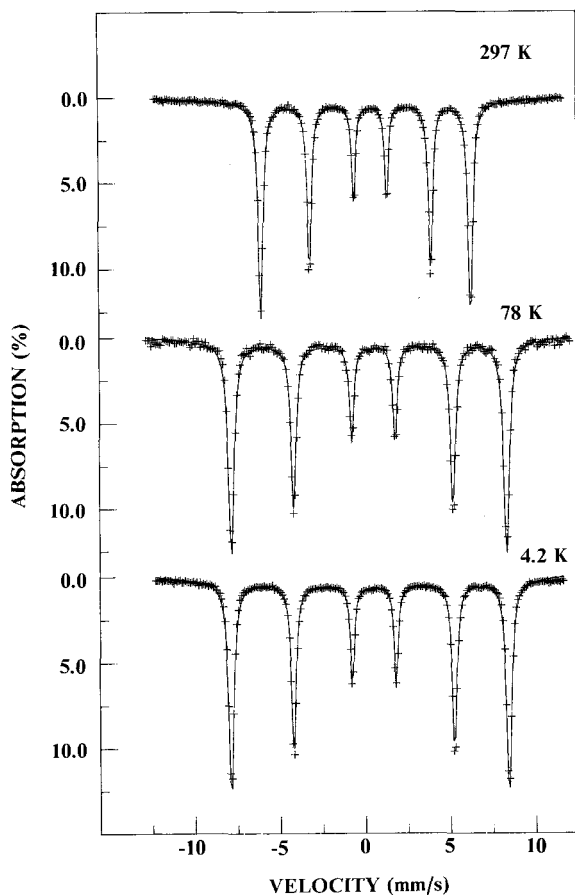


Figure 3. Mössbauer spectra of a highly crystalline natural goethite obtained at 297, 78, and 4.2 K.

order as the crystallinity decreased. As seen in Figure 5, the Mössbauer spectrum of preparation 3, which contains 4% Si per Fe (i.e., 4 Si atoms per 100 Fe) has a weak ordered component at room temperature, as well as a strong quadrupole doublet.

Initially, each Si-containing product was studied at room temperature, 78, and 4.2 K. These spectra suggest that the ordering temperature decreased with increasing Si content until in preparations 6, 7, and 8 (containing 8 to 12% Si) the magnetic ordering was only apparent at 4.2 K. The only striking difference between the Mössbauer spectra of the more highly incorporated materials is the small magnetic component observed at 78 K in preparations 4 and 5, which is probably due to the method of preparation. In method I, the alkaline solutions were aged before the addition of Na_2HPO_4 or Na_2SiO_3 (see Experimental section). During this aging period nuclei of goethite crystals formed in the suspension and subsequently acted as growth site seeds in the main precipitation stage after the addition of the Na_2HPO_4 or Na_2SiO_3 . At high Na_2HPO_4 or Na_2SiO_3 concentrations this nucleated growth was non-uniform.

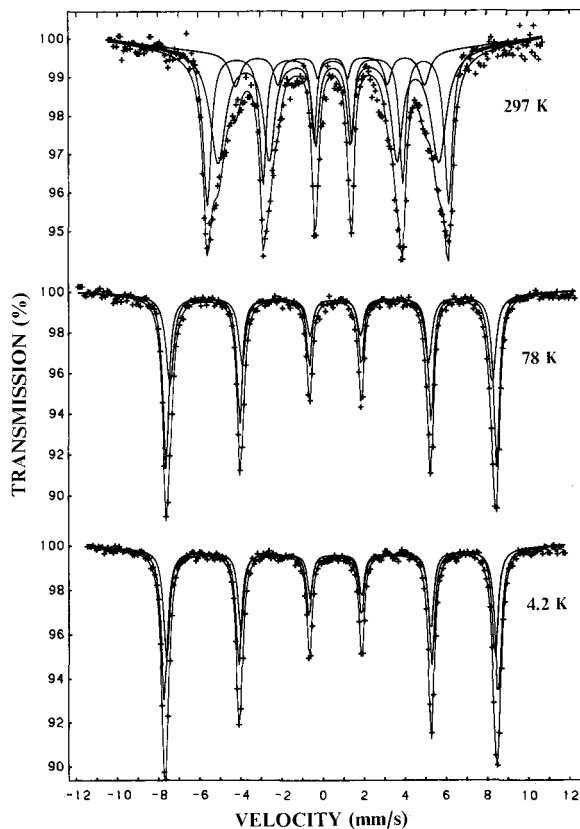


Figure 4. Mössbauer spectra of preparation 1 obtained at 297, 78, and 4.2 K.

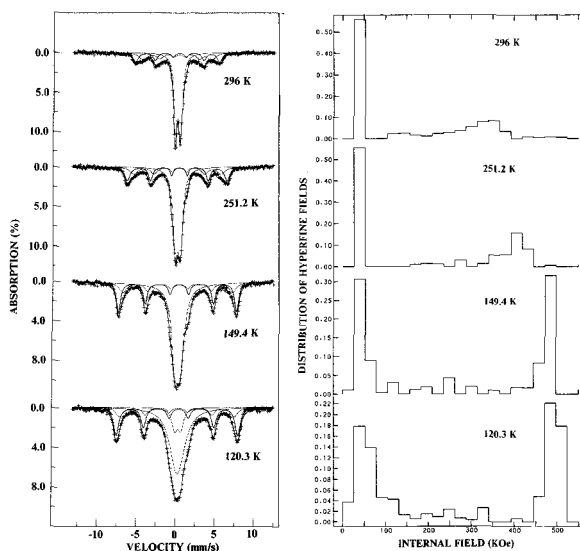


Figure 5. (A) Mössbauer spectra of preparation 3 obtained between 296 and 120.3 K. (B) Corresponding hyperfine field distributions. Components present at less than 100 kOe do not represent actual fields but indicate contributions from (superparamagnetic) quadrupole doublets present.

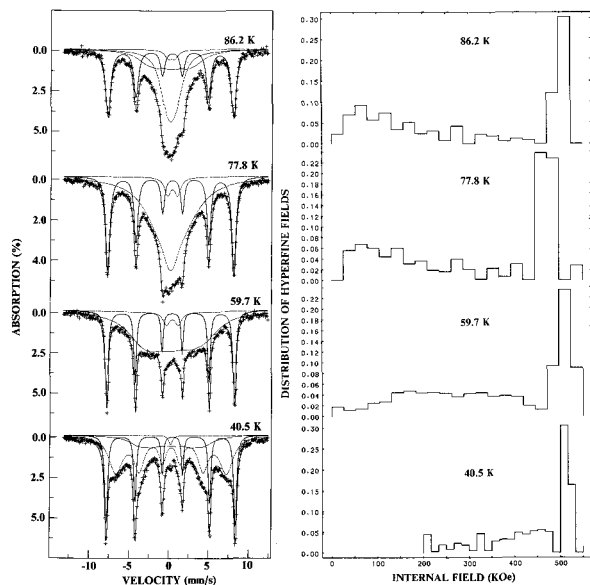


Figure 6. (A) Mössbauer spectra of preparation 3 obtained between 86.2 and 40.5 K. (B) Corresponding hyperfine field distribution.

On the basis of Mössbauer results obtained at room temperature, 78, and 4.2 K, we decided to investigate in detail the temperature dependence of the hyperfine fields in preparations 3 and 6. Selected results for preparation 3 (containing 4% Si) and 6 (containing 8.6% Si) are given in Figures 5–7 and 8 and 9, respectively. In preparation 3, two differences were noted: (1) beginning at 296 K, the quadrupole doublet decreased in intensity and a concomitant magnetic sextet grew in

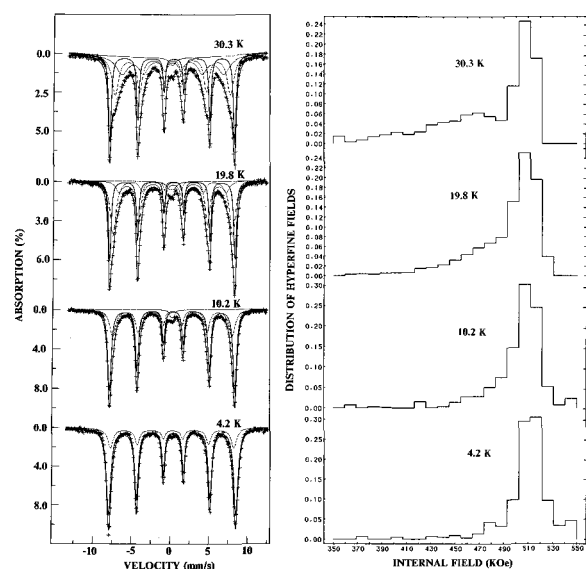


Figure 7. (A) Mössbauer spectra of preparation 3 obtained between 30.3 and 4.2 K. (B) Corresponding hyperfine field distributions.

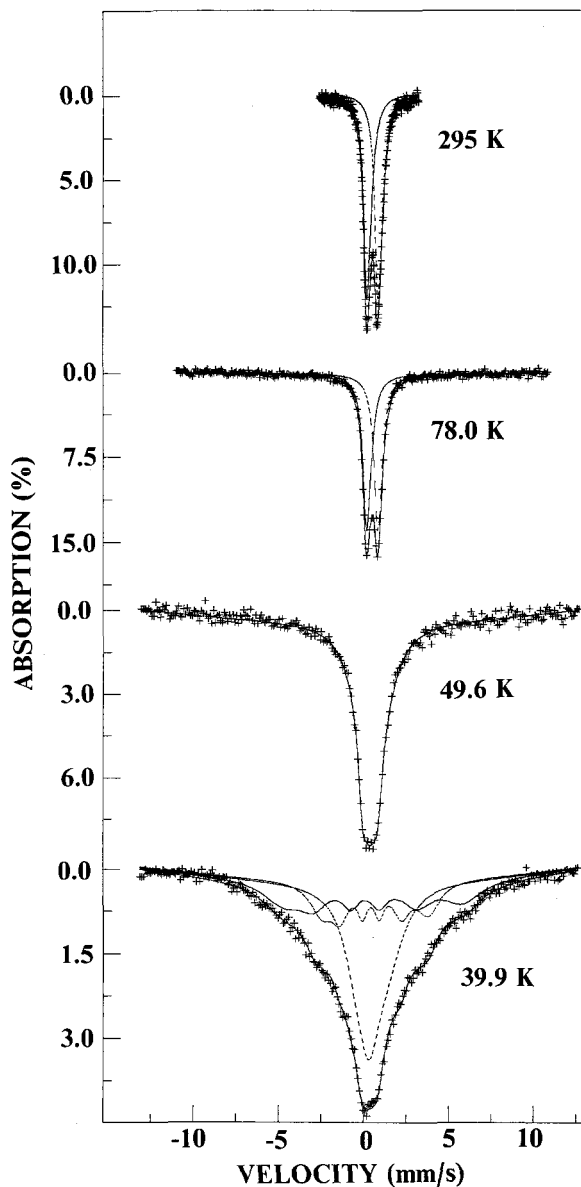


Figure 8. Mössbauer spectra of preparation 6 obtained between 295 and 39.93 K.

intensity with temperature (see Figure 5); and (2) at about 150 K a single broad peak, representing a magnetic component undergoing rapid relaxation on the Mössbauer timescale, was present and increased in width with temperature until it separated into a resolved sextet at ~ 50 K (Figure 6). At lower temperatures (Figure 7) the unordered component was absent, and a sharper distribution of internal hyperfine fields was present. The broad peak probably does not represent a specific phase, but rather a range of crystal sizes each having a different amount of incorporated Si. Preparation 6 behaved differently in that no ordered magnetic component was observed at ≥ 78 K (Figure

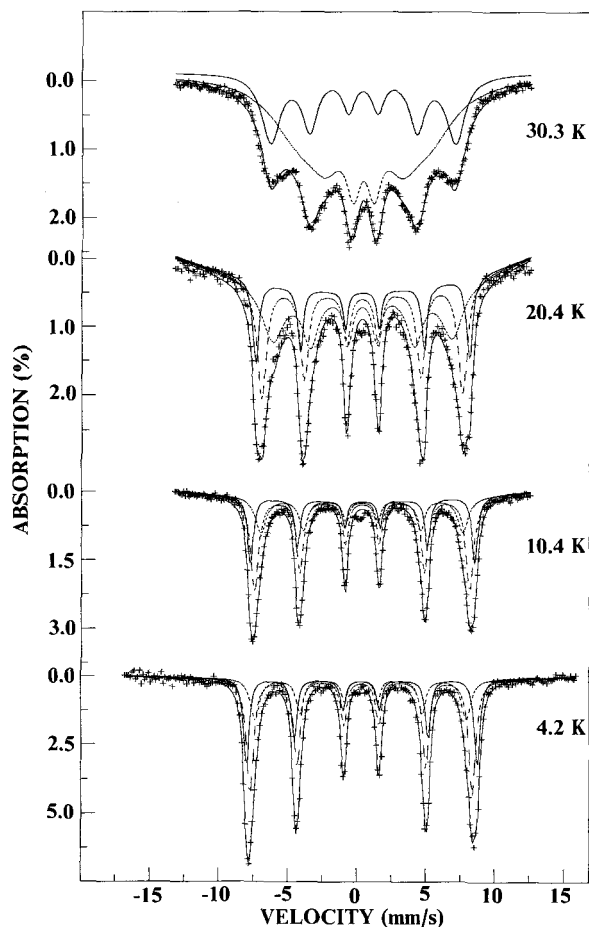


Figure 9. Mössbauer spectra of preparation 6 obtained between 30.32 and 4.2 K.

8). At temperatures < 65 K the internal hyperfine field gradually increased with decreasing temperature, until at ≤ 30 K (see Figure 9) a broad magnetic sextet was present.

Similarly, in materials incorporating P, the temperature at which magnetic ordering appeared fell rapidly as the P:Fe ratio increased. Although all samples showed well-resolved magnetic sextets at 4.2 K, the linewidths were greater than those of the preparations containing Si. Here also, the samples prepared by method I, after aging, showed a weak magnetic sextet at higher temperature, whereas those prepared by method II showed no such component (see Figures 10 and 12).

The importance of this aging step on the magnetic properties of the product is clearly revealed by the temperature dependence of the spectra obtained for preparations 10 and 12. Preparation 10, having a P:Fe ratio of 3.5:100 and prepared by method II with no aging and no prior formation of goethite nuclei and seeds, showed a slow increase in the internal field with decreasing temperature (Figures 10 and 11). This behavior is similar to that of preparation 6 (Figures 8

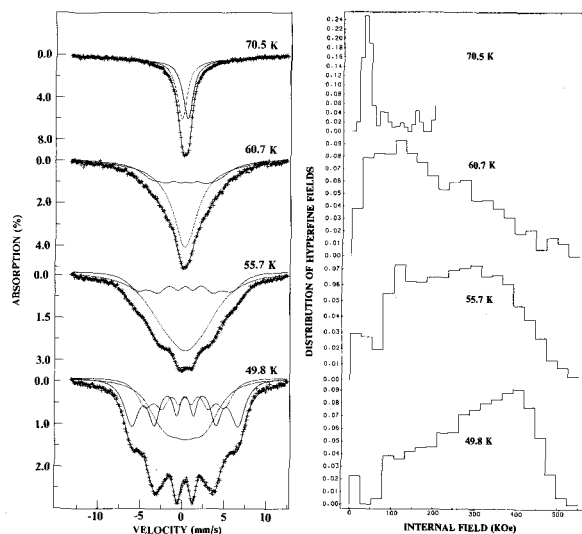


Figure 10. (A) Mössbauer spectra of preparation 10 obtained between 70.5 and 49.8 K. (B) Corresponding hyperfine field distributions. The components present at less than 100 kOe do not represent actual fields, but indicate contributions from (superparamagnetic) quadrupole doublets present.

and 9) also prepared by method II. In contrast, preparation 12 (containing 6% P), which was aged as part of method I, contained microcrystalline goethite whose magnetic spectrum is apparent at 97.7 K (see Figure 12). For this preparation, the intensity of this magnetic component increased with decreasing temperature. Simultaneously, a broad line corresponding to a large distribution of hyperfine fields or broadened magnetic relaxation appeared and gradually broadened at tem-

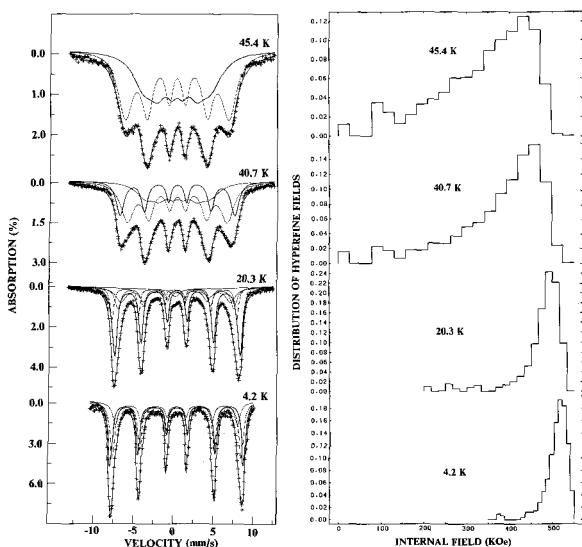


Figure 11. (A) Mössbauer spectra of preparation 10 obtained between 45.4 and 4.2 K. (B) Corresponding hyperfine field distributions.

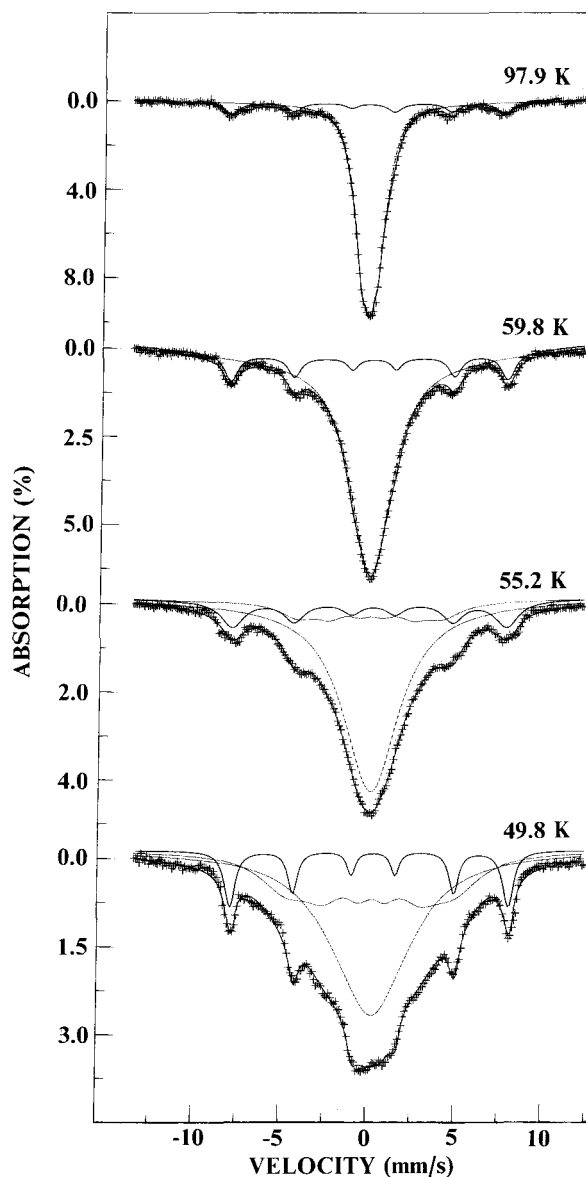


Figure 12. Mössbauer spectra of preparation 12 obtained between 97.7 and 49.8 K.

peratures <60 K to give an internal field at 4.2 K, similar to that of pure goethite.

DISCUSSION

The incorporation of small amounts of Si or P (as little as 3%) during the preparation of synthetic goethites yielded products which contained similar amounts of water as synthetic goethite, but which differed in physical properties. The presence of larger amounts of Si or P during the synthesis resulted in mixtures that had water contents similar to that of goethite, but showed further differences from goethite in their physical properties.

In the absence of Si and P, the hydrolysis of aqueous

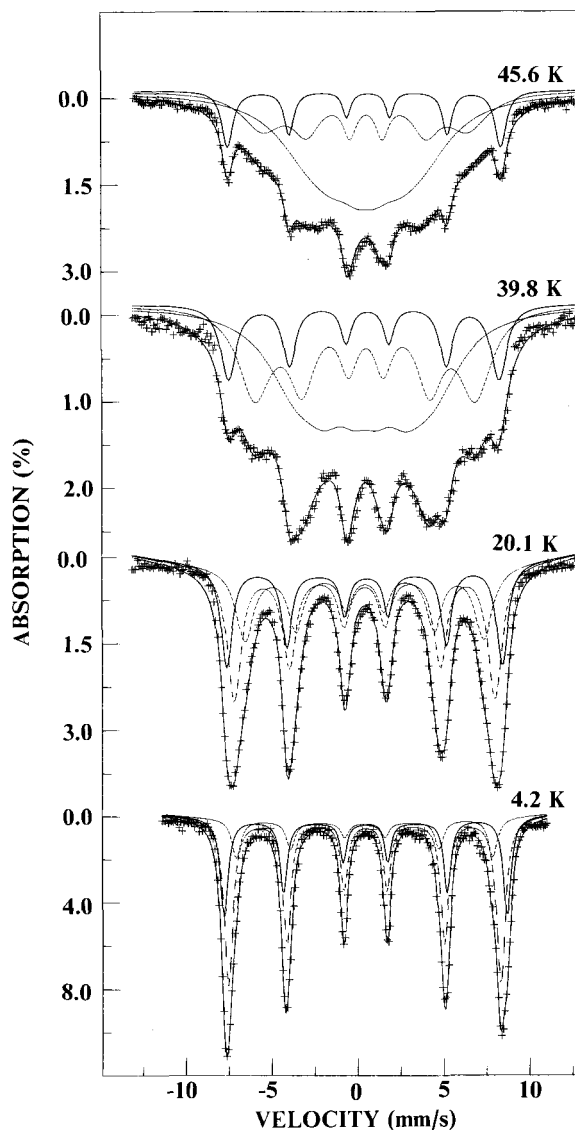


Figure 13. Mössbauer spectra of preparation 12 obtained between 45.6 and 4.2 K.

Fe^{3+} complexes gave oligomeric and polymeric forms which then precipitated out of solution as ferrihydrite. This material then redissolved at high pH allowing goethite to precipitate by successive addition of aqueous Fe^{3+} hydroxide complexes, e.g., $\text{Fe}(\text{OH})_4^-$. The decrease in crystallinity indicates that Si and P did not substitute for Fe in the crystal structure of goethite. Direct substitution of the Si or P for Fe would have led to materials exhibiting goethite XRD patterns, perhaps with differing lattice parameters. Rather, at least at these high pH values, by adsorption on growth sites the Si and P restricted crystallite size, forced irregularities in crystal growth, and ultimately (at high Si and P concentrations) prevented the formation of goethite. Although many of the products contained ferrihydrite

Table 2. Mössbauer-effect spectral parameters obtained from fits with discrete components.¹

Preparation	δ_{ave}			ΔE_Q		H_{int} (ave)	
	295 K	78 K	4.2 K	295 K	~295 K	78 K	4.2 K
Natural	0.38	0.49	0.50	—	380	500	505
1	0.40	0.50	0.50	—	339	493	500
2	0.38	0.47	0.51	0.63	247	487	506
3	0.35	0.48	0.49	0.64	81	231	492
4	0.34	0.45	0.47	0.68	0	14	481
5	0.34	0.41	0.46	0.70	0	0	497
6	0.33	0.44	0.46	0.65	0	0	497
7	0.33	0.48	0.49	0.64	0	374	486
8	0.34	0.45	0.46	0.69	0	0	494
9	0.38	0.51	0.51	—	325	492	504
10	0.35	0.45	0.48	0.64	0	0	496
11	0.33	0.45	0.48	0.63	0	0	493
12	0.34	0.46	0.49	0.63	0	40	488
13	0.34	0.44	0.48	0.65	0	0	498
14	0.32	0.43	0.47	0.66	0	0	498

¹ All data in mm/s; δ_{ave} is relative to room-temperature natural α -iron foil. H_{int} is in kOe. Average values given are area-weighted averages.

(as shown by microbeam electron diffraction), they still yielded goethite-like Mössbauer hyperfine parameters. For example, the 515-kOe maximum in the distribution of fields observed at 4.2 K for preparation 10 was similar to that for pure goethite (Mørup *et al.*, 1983; Quin, 1986) and substantially larger than the ~480-kOe field found for ferrihydrite (Quin, 1986). The hyperfine field distribution (Figure 11B) is consistent with the presence of about 20% ferrihydrite in this material, as indicated by microbeam electron diffraction (see Table 1).

Goethite, substituted goethite, and related materials have been the subject of numerous Mössbauer studies (see, e.g., Fysh and Clark, 1982; Murad and Schwertmann, 1983; Mørup *et al.*, 1983; and references therein). The unusual lineshape observed in the low-temperature magnetic spectra of synthetic and poorly crystalline natural goethite have been studied in detail, most recently by Mørup *et al.* (1983) who proposed a "superferromagnetism" model based upon a modified Weiss mean-field theory for interacting particles. Quin (1986) obtained almost identical spectral results for several natural and undoped synthetic goethites. Recent work on Al-goethites (Fysh and Clark, 1982; Murad and Schwertmann, 1983) showed that the internal hyperfine field decreased by 0.5 kOe per mole % Al. At 20 mole % Al the field was reduced to 495 kOe; however, the hyperfine field distribution and temperature dependence of the spectra were similar to those of both natural or microcrystalline goethite. In contrast, the samples examined here gave different spectral properties and hyperfine field distributions.

The general similarity of many of our synthetic materials to goethite is supported by their Mössbauer hyperfine parameters. The isomer shift values, δ , obtained at low temperatures (see Tables 2 and 3) were nearly identical to the value of 0.48 ± 0.01 mm/s obtained

at 10 K for natural, highly crystalline goethite (Mørup *et al.*, 1983). Furthermore, the range of average values at 4.2 K of the quadrupole shifts of -0.10 to -0.15 mm/s agrees well with the value of -0.12 ± 0.01 mm/s obtained at 10 K. As expected (see Fysh and Clark, 1982), Si or P had a more pronounced influence on the average internal hyperfine field observed at 4.2 K. The natural goethite examined here gave a value of 509 kOe, the pure synthetic goethite, a value of 504 kOe, and the incorporated samples, a mean value of 502 kOe with a standard deviation of 6 kOe. These values compare well with the saturation value of 506 ± 1 kOe obtained by Mørup *et al.* (1983) for natural goethite and the range of lower values reported by Fysh and Clark (1982) and Murad and Schwertmann (1983) for a series of Al-substituted goethites.

The data reported herein indicate a breakdown in long-range structural and magnetic order even if some small microcrystallites were present as aggregates resembling the acicular shape of pure goethite crystals (Cornell *et al.*, 1983). In other samples, the goethite nuclei and subsequent seeds that formed during the aging step of method I appear to be in an aggregate of doped ferrihydrite and non-diffracting material. The materials containing the largest amount of incorporated Si and P were almost completely noncrystalline, i.e., from X-ray powder and electron diffraction results, they showed no order at the lowest level of resolution, ~ 10 Å.

At very low incorporation levels, as in preparations 2 and 9 which contained $<2.5\%$ Si or P, the magnetic properties and, hence, the Mössbauer spectra were similar to those of the poorly crystalline natural or synthetic goethites (see Figure 4). For the products containing large amounts of Si or P and which were not aged (i.e., prepared by method II), no evidence of order was found at temperatures >65 K. At lower temper-

atures, a broader Mössbauer spectrum was found (see Figures 8 and 10 for Si- and P-incorporated samples, respectively), due to the slowing of the magnetic relaxation on several different Fe sites in these poorly crystalline materials. At <20 K the relaxation was slow, and a typical magnetic sextet Mössbauer spectrum was observed. As shown in Figures 9 and 11, however, the linewidth of the spectrum was much greater than that found for natural goethite (see Figure 3), probably due to the variety of sites and, hence, hyperfine fields and moments in these materials. The different iron sites in the samples are indicated by the components shown in the Mössbauer spectra and by the width of the hyperfine field distribution.

As seen in Tables 1–3 the samples prepared by method I (i.e., with aging) were different from those prepared by method II in that an ordered magnetic component was present either at room temperature, as shown in Figure 3 (Si-incorporated preparation 3) or at 97.7 K as shown in Figure 12 (P-incorporated preparation 12). The magnetic component in preparation 12 was observed at ~140 K and coexisted with a fully developed internal hyperfine field, more or less equivalent to that expected (see Mørup *et al.*, 1983) for poorly crystalline goethite. Furthermore, this magnetic component increased in intensity, and the quadrupole doublet component decreased in intensity with decreasing temperature (Figures 5, 6, and 12). Such behavior is indicative of superparamagnetism (Chukhrov, 1973), with rapid fluctuation of the magnetization above the blocking temperature. Unfortunately, the average blocking temperature could not easily be determined, because at lower temperature the spectra were further complicated by the presence of slow magnetic relaxation, which gave rise to a broad spectral component similar to that discussed above for preparations 6 and 10. The combination of these features indicates a range of crystallite sizes and hence of blocking temperatures. At 4.2 K all of the samples prepared by method I gave similar spectra.

At room temperature as much as 50% of preparation 3 exhibited long-range magnetic order. This was unexpected because this material contained at most a trace of crystalline goethite, as estimated by microbeam electron diffraction. The ferrihydrite would not be ordered at >60 K (Quin, 1986). The “seed” crystals were apparently more influential on the magnetic properties than was expected. These microcrystals probably extended their influence into their surrounding aggregate of doped noncrystalline material in a fashion similar to that proposed by Mørup (1987) for coupling between adjacent microcrystals in microcrystalline goethite.

In conclusion, the magnetic properties observed in the Mössbauer spectra, i.e., the ordering temperature, as reflected in the relaxation rate, and/or the blocking temperature decreased with increasing Si or P incor-

Table 3. Mössbauer-effect hyperfine parameters obtained from the field distribution.¹

Preparation	T(K)	δ (mm/s)	H_{ave}	H_{max}	H_{max}^2	% Non-magnetic
1	296	0.47	332	375	356	nil
	78	0.50	497	503	497	nil
	4.2	0.47	504	535	503	nil
2	296	0.45	280	370	351	14
	78	0.45	494	497	489	10
	4.2	0.50	510	513	510	nil
3	296	0.33	143	360	331	57
	251	0.36	166	410	393	58
	200	0.39	208	460	437	55
	149.4	0.41	231	480	465	57
	120.3	0.47	245	480	481	57
	100.2	0.47	269	510	483	50
	86.2	0.48	284	510	487	45
	77.8	0.46	293	515	489	5
	59.7	0.53	346	510	495	5
	50.2	0.50	383	515	497	nil
40.5	0.49	444	515	501	nil	
30.3	0.49	473	510	500	nil	
19.8	0.49	485	510	501	nil	
10.2	0.49	498	510	501	nil	
4.2	0.49	507	512	502	nil	
5	4.2	0.47	501	512	517	nil
6	49.6	0.47	72	230	47	nil
	39.9	0.47	188	430	326	nil
	30.3	0.47	316	440	415	nil
	20.4	0.47	433	475	480	nil
	10.4	0.47	481	510	485	nil
	4.2	0.47	504	517	506	nil
7	4.2	0.47	490	504	499	nil
8	4.2	0.47	498	512	506	nil
9	296	0.47	325	365	349	nil
	78	0.50	495	502	493	nil
	4.2	0.50	509	512	507	nil
10	65.0	0.45	117	200	152	41
	60.7	0.44	183	295	244	nil
	55.7	0.47	240	340	345	nil
	49.8	0.46	290	390	391	nil
	45.4	0.46	332	425	402	nil
	40.7	0.46	366	450	445	nil
	30.1	0.46	419	475	478	nil
	20.3	0.46	469	487	486	nil
	10.2	0.46	491	505	513	nil
	4.2	0.49	507	520	513	nil
12	97.7	0.43	86		484	nil
	59.6	0.47	194		491	nil
	55.2	0.47	220		486	nil
	49.6	0.47	266	500	493	nil
	45.6	0.47	305	508	492	nil
	39.8	0.47	343	508	488	nil
	35.2	0.48	375	508	495	nil
	20.1	0.51	470	492	496	nil
	10.0	0.49	492	507	505	nil
	4.2	0.49	496	507	510	nil
14	4.2	0.50	501	517	507	nil

¹ δ is relative to room-temperature α -iron foil and the fields are given in kOe.

² As determined from the component fits.

poration. This decrease was probably due to the extensive loss of crystallinity (see above) that accompanied the Si or P incorporation, the effect being greater for P than for Si. This loss suggests that Si and P did not replace Fe in the goethite structure. Such a replacement would have resulted in drastic reductions in the Si saturation hyperfine field. Instead, the Si and P must have been adsorbed strongly on crystal growth sites. It will be interesting to study natural materials from both mineral and biological sources to see how they behave when examined in this way.

ACKNOWLEDGMENTS

The authors thank S. Mørup, F. Grandjean, M. Thomas, C. E. Johnson, D. P. E. Dickson, A. K. Cheetham, and T. St. Pierre for many stimulating and enjoyable conversations during the course of this work and D. E. Tharp for help with the hyperfine-field distribution fits. We also thank Daresbury Laboratory for the use of their computing facilities and the Royal School of Mines for samples of natural goethite. GJL thanks the donors of the Petroleum Research Fund, administered by the American Chemical Society, for their support of this research and the United Kingdom Science and Engineering Research Council for a Faculty Research Fellowship during a sabbatical visit at the University of Liverpool.

REFERENCES

- Atkinson, R. J., Posner, A. M., and Quirk, J. P. (1968) Crystal nucleation in Fe(III) solutions and hydroxide gels: *J. Inorg. Nucl. Chem.* **30**, 2371–2381.
- Böhm, J. (1925) Aluminum hydroxide and iron hydroxide: *Z. Anorg. Allgem. Chem.* **149**, 203–216.
- Cheetham, A. K. and Skarnulis, A. J. (1981) X-ray microanalysis of thin crystals in the electron microscope and its application to solid state chemistry: *Anal. Chem.* **53**, 1060–1064.
- Chukhrov, F. V. (1973) On mineralogical and geochemical criteria in the genesis of red beds: *Chem. Geol.* **12**, 67–75.
- Cornell, R. M., Mann, S., and Skarnulis, A. J. (1983) A high-resolution electron microscopy examination of domain boundaries in crystals of synthetic goethite: *J. Chem. Soc. Faraday Trans. 1*, **79**, 2679–2684.
- Cornell, R. M. and Schwertmann, U. (1979) Influence of organic anions on the crystallization of ferrihydrite: *Clays & Clay Minerals* **27**, 402–410.
- Fysh, S. A. and Clark, P. E. (1982) Aluminous goethite: A Mössbauer effect study: *Phys. Chem. Minerals* **8**, 180–187.
- Fysh, S. A. and Fredericks, P. M. (1983) Fourier transform infrared studies of aluminous goethite and hematites: *Clays & Clay Minerals* **31**, 377–382.
- Goldztaub, M. S. (1935) Study of some derivatives of ferric oxide (FeOOH, FeO₂Na, FeOCl); determination of their structures: *Bull. Soc. Franc. Mineral.* **58**, 6–76.
- Koch, C. J. W., Madsen, M. B., Mørup, S., Christiansen, G., Gerward, L., and Villadsen, J. (1986) Effect of heating on microcrystalline synthetic goethite: *Clays & Clay Minerals* **34**, 17–24.
- Longworth, G. (1984) Spectral data reduction and refinement: in *Mössbauer Spectroscopy Applied to Inorganic Chemistry*, Vol. 1, G. J. Long, ed., Plenum Press, New York, 43–56.
- Mann, S. (1983) Mineralization in biological systems: *Structure and Bonding* **54**, 125–174.
- Mann, S., Cornell, R. M., and Schwertmann, U. (1985) The influence of aluminium on iron-oxides. 12. High-resolution transmission electron-microscopic (HRTEM) study of aluminous goethite: *Clay Miner.* **20**, 255–262.
- Mann, S., Perry, C. C., Webb, J., Luke, B., and Williams, R. J. P. (1986) Structure, morphology, composition and organization of biogenic minerals in limpet teeth: *Proc. Royal Soc. B (London)* **227**, 179–190.
- Mørup, S. (1987) Industrial applications of Mössbauer spectroscopy to microcrystals: in *Industrial Applications of the Mössbauer Effect*, G. J. Long and J. G. Stevens, eds., Plenum Press, New York, 63–81.
- Mørup, S., Dumesic, J. A., and Topsøe, H. (1980) Magnetic microcrystals: in *Applications of Mössbauer Spectroscopy*, Vol. 2, R. L. Cohen, ed., Academic Press, New York, 1–53.
- Mørup, S., Madsen, M. B., Franck, J., Villadsen, J., and Koch, C. J. W. (1983) A new interpretation of Mössbauer spectra of microcrystalline goethite: “Super-ferromagnetism” or “super-spin-glass behaviour?": *J. Mag. Mag. Materials* **40**, 163–174.
- Murad, E. and Johnston, J. H. (1987) Iron oxides and oxyhydroxides: in *Mössbauer Spectroscopy Applied to Inorganic Chemistry*, Vol. 2, G. J. Long, ed., Plenum Press, New York, 507–582.
- Murad, E. and Schwertmann, U. (1983) The influence of aluminium substitution and crystallinity on the Mössbauer spectra of goethite: *Clay Miner.* **18**, 301–312.
- Quin, T. G. (1986) Aspects of the biomineralisation of iron: D. Phil. Thesis, Oxford University, Oxford, United Kingdom, 231 pp.
- Russell, J. D. (1979) Infrared spectroscopy of ferrihydrite: Evidence for the presence of structural hydroxyl groups: *Clay Miner.* **14**, 109–114.
- Schulze, D. G. (1984) The influence of aluminum on iron oxides. VIII. Unit-cell dimensions of Al-substituted goethites and estimation of Al from them: *Clay & Clay Minerals* **32**, 36–44.
- Schwertmann, U. and Fischer, W. R. (1966) Zur Bildung von α -FeOOH und α -Fe₂O₃ aus amorphem Eisen(III)-hydroxide. III: *Z. Anorg. Allg. Chem.* **346**, 137–142.
- Schwertmann, U. and Thalmann, H. (1976) The influence of Fe(III), Si and pH on the formation of lepidocrocite and ferrihydrite during oxidation of aqueous FeCl₂ solutions: *Clay Miner.* **11**, 189–200.
- Shannon, R. D. and Prewitt, C. T. (1969) Effective ionic radii in oxides and fluorides: *Acta Crystallogr.* **B25**, 925–946.
- Taylor, R. M. and Schwertmann, U. (1974) Association of phosphorus with iron in ferruginous soil concretions: *Aust. J. Soil Res.* **12**, 133–145.
- Towe, K. M. and Bradley, W. F. (1967) Mineralogical constitution of colloidal “hydrrous ferric oxides”: *J. Coll. Interfacial Sci.* **24**, 384–392.
- van Oosterhout, G. W. (1960) Morphology of synthetic submicroscopic crystals of α and β -FeOOH and of α -Fe₂O₃ prepared from FeOOH: *Acta Crystallogr.* **13**, 932–935.
- Wivel, C. and Mørup, S. (1981) Improved computational procedure for evaluation of overlapping hyperfine parameter distributions in Mössbauer spectra: *J. Phys. E. Sci. Instrum.* **14**, 605–610.

(Received 24 November 1986; accepted 5 December 1987; Ms. 1623)